VOL 5, NO.1 (March 2025) 34-56
https://jagst.utm.my

Journal of Advanced Geospatial Science & Technology

Long-Term Coastal Erosion Vulnerability Assessment in Kuala Rompin Using Remote Sensing (2003-2023)

Nur Zahirah Azziddin, Kelvin Tang Kang Wee*
Geomatic Innovation Research Group (GnG), Faculty of Built Environment & Surveying,
Universiti Teknologi Malaysia, 81310 Johor Bahru, Johor, Malaysia

Corresponding author: kkelvin@utm.my

Abstract – Coastal erosion is a severe environmental threat, impacting many coastal areas worldwide. The increasing rate and severity of erosion occurrences can be attributed to natural and human sources. Coastal erosion is becoming more prevalent through rising sea levels, climate change, and human activities, including urbanisation and unsustainable coastal development. This study examines the geographical and chronological patterns of coastal erosion along the shoreline of Kuala Rompin, Pahang, for a long-term period, specifically from 2003 to 2023. Over the past twenty years, coastline features and coastal erosion rates have been revealed by utilising Landsat satellite optical imagery. Additionally, with the desired satellite revisit timeframe, the combination of high-resolution multispectral data and advanced GIS spatial analysis tools enables comprehensive change detection to assess the coastal landscape's dynamic pattern and vulnerability rate. Data analysis indicates an average erosion rate of -0.476 meters per year, with significant variability along the coastline. Besides that, this study also delved deeper into the relationship between environmental factors and the likelihood of erosion, offering valuable insights into the factors that caused changes in the coastal area. The utilisation of GIS and remote sensing images in this study provided a flexible and adaptable framework in the form of classified remote sensing images and GIS models complete with analysis for evaluating the susceptibility of coastal areas in different regions, promoting a wider range of potential applications for the research findings to aid other departments in mitigating and preventing coastal erosion in the area. The findings provide an enhanced comprehension of the dynamics of coastal erosion around Kuala Rompin, facilitating well-informed decision-making for implementing sustainable methods in coastal management. In summary, this research can serve as a significant reference for environmental scientists, policymakers, and coastal management practitioners involved in addressing the effects of erosion on susceptible coastal regions.

Keywords *– Coastal erosion, GIS, Remote sensing*

Article History: Received 6 October 2024, Accepted 28 February 2024, Published 28 March 2025

How to cite: Azziddin, N. Z. and Tang, K. W. K. (2025). Long-Term Coastal Erosion Vulnerability Assessment in Kuala Rompin Using Remote Sensing (2003-2023). Journal of Advanced Geospatial Science & Technology. 5(1), 34-56.

1.0 Introduction

According to the Luijendijk *et al.* (2018), the coastline is a barrier that divides the water from the mainland. They stated that the term "coastal zone" can refer to the larger geographical area where the worldwide sea meets land. Rock coastlines, extensive mangrove forests, and muddy salt marshes are examples of coastal zones. Mahmud & Tang (2023) has stated that Malaysia has a total land area of 332,556 km^2, with 4,800 km comprising coastlines due to Malaysia's territorial seas encompassing about 150,000 km^2.

The process by which the local sea-level rise, intense wave movement, and coastal flooding tear down or sweep away rocks, soils, and/or sands along the shore is known as coastal erosion, as stated by the Masselink & Gehrels (2014), and other natural phenomena create erosion across all coastlines along with the combination of the effects of storm surges at high tide with additional impacts from large waves creates the most devastating scenarios. Due to the ever-growing effects of climate change and global warming, there has been an alarming increase in hazards affecting Malaysia's shorelines, bringing about coastal erosion and an escalation of sea-level rise (Mohamed Rashidi *et al.*, 2021). Hasan *et al.* (2023) has reported that 1,347.6 km of an 8,840 km coastline is actively eroding, with one-third of the area dropping into the critical and major categories that require structural protection. This is hazardous to the coastline mainly because, as a maritime country, Malaysia is situated near the equator in Southeast Asia, with key ports on international marine and shipping routes. Seven water zones enclose it, and the total sea area is about double the land area (Flewwelling *et al.*, 2021). As a result, the threats of coastal erosion and sea-level rise have continually negatively affected the physical, socioeconomic, and biodiversity along the coastlines.

The coastline is an ever-changing setting where human constructions and activities are situated. As a result, it is critical to have a reliable instrument to measure, estimate, and, if possible, predict shoreline movement towards the land or toward the ocean (Apostolopoulos, 2021). Therefore, Geographical Information Systems (GIS), as well as satellite images obtained from remote sensing, have been used for a prolonged amount of time to monitor the positioning of shore zones and coastline, which can provide consistent and accurate statistics of coastal fluctuations (Yasir *et al.*, 2020, Hussaini *et al.*, 2020).

This study stands out by employing a novel approach to coastal erosion assessment by integrating multispectral satellite images and cloud-based processing. The Google Earth Engine

(GEE) platform allows for extensive geospatial analysis and visualisation in predicting disease outbreaks. It provides a robust framework for remote sensing research and natural resource management. Key highlights include utilising the cloud-based GEE platform for a detailed assessment of coastal erosion vulnerability and coastal fluctuations rate along Kuala Rompin's shoreline over an extended period from 2003-2023. This approach addresses current gaps in coastal monitoring methodologies, offering consistently accurate statistics on coastal fluctuations. This, in turn, aids in effective coastal management and decision-making, contributing to the body of knowledge with a more sophisticated and precise method of assessing and managing coastal erosion in Malaysia.

2.0 Method and Area

2.1 Shoreline Delineation

The initial step of the flowchart in this research, as shown in Figure 1 below, involved carrying out a preliminary study and identifying the study area. Based on past relevant research studies, the goals and research challenges were defined and established at this study stage. The research focused on the issue of coastal erosion in a research area situated along the coast of Kuala Rompin, Peninsular Malaysia, based on the presence of tangible evidence that indicated a portion of the shoreline eroded since the 2010s. This eased the process of displaying the rate of shoreline changes and the conspicuous indications of coastal erosion around that area.

The data for this study was retrieved from the GEE cloud-based platform that provided the past and latest satellite imagery intended to enhance the knowledge of the extent and pattern of coastal erosion in the coastline region of Kuala Rompin (Figure 2). This research has used a unique and comprehensive method to discover, analyse and predict the erosion rate of the Kuala Rompin area over 20 years, from 2003 until 2023. The references suggest a monitoring period of at least 20 years can be considered long-term (Turner *et al.*, 2016; Castelle & Harley, 2020). This extended timeframe allows researchers to capture the natural variability and cyclical patterns of coastal processes and detect the gradual, cumulative impacts of climate change, sea-level rise, and human activities on the coastline (McClenachan *et al.*, 2020).

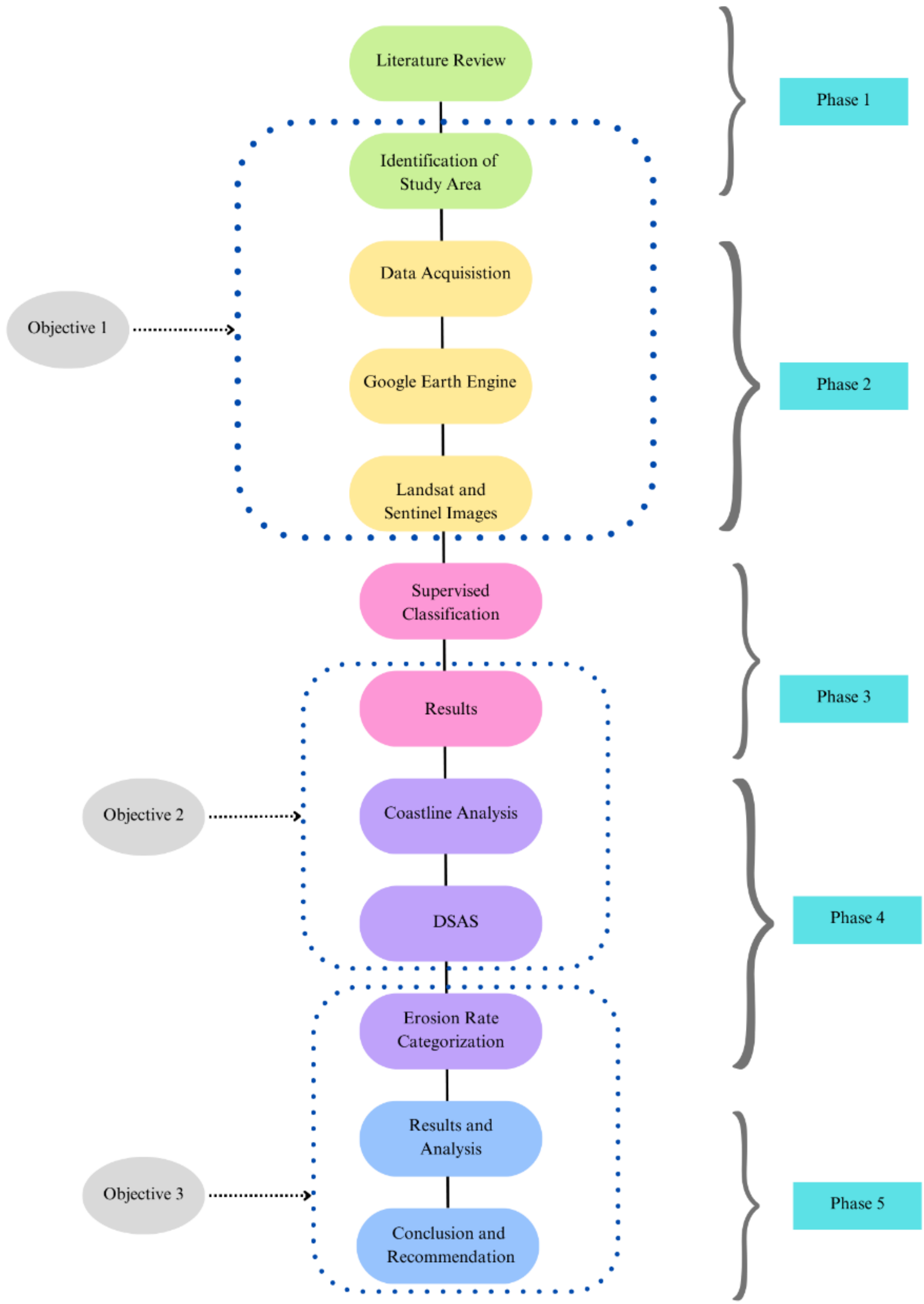

Figure 1. Workflow for this research's methodology

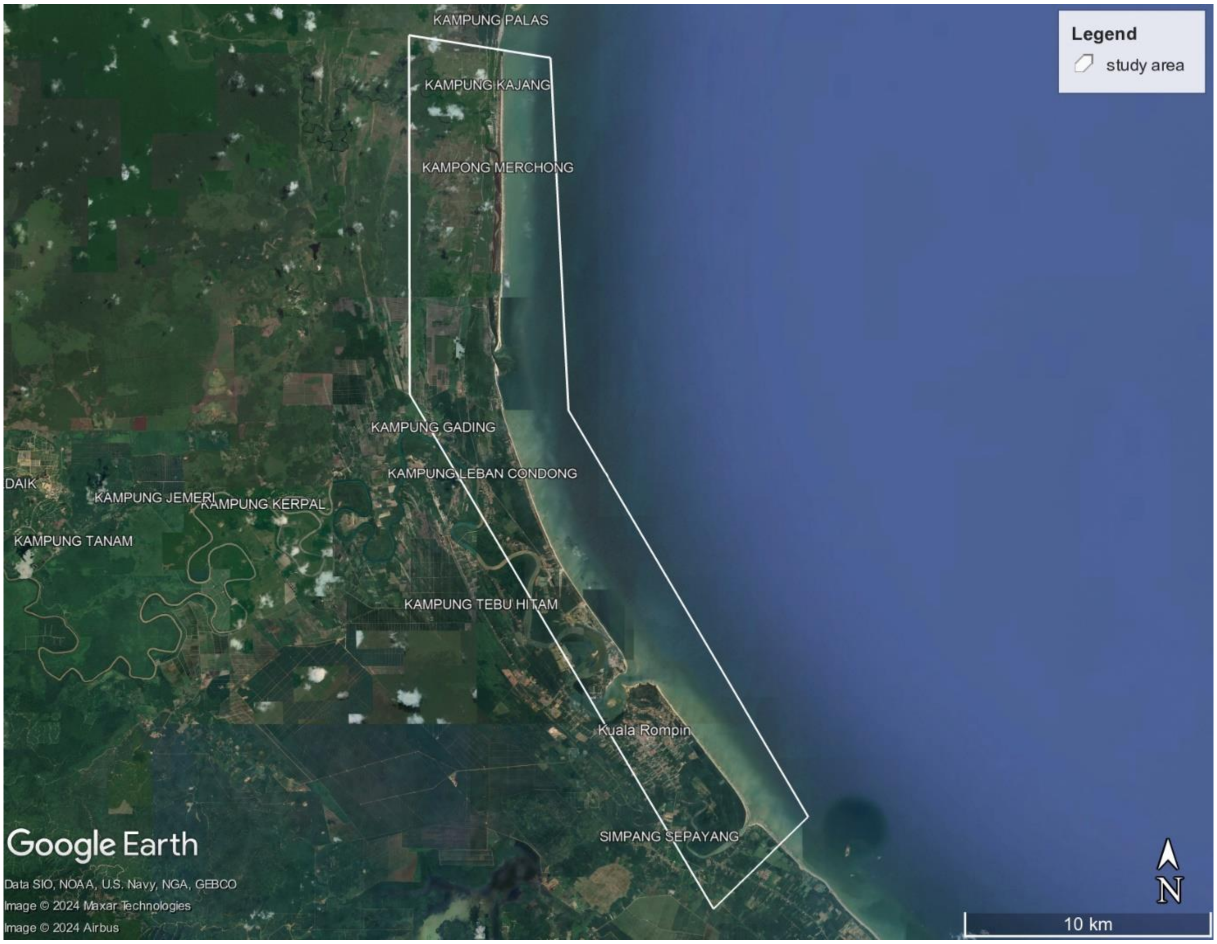

Figure 2. The study area of this research (Google Earth, 2024)

Upon defining the work area, the next step involved examining the preceding study conducted in the research paper, articles, journals, websites, and other relevant sources regarding coastal erosion, remote sensing images, shoreline analysis, and classification. The study table has resulted in a comprehensive compilation of reviews from prior research, whereas this chapter will provide a clear definition of all methodologies, formulae, and statistical measures used.

The second phase included the collection of data. This research used data obtained from remote sensing to carry out the coastal analysis. The research used data spanning 20 years, from January 2003 to December 2023, consisting of yearly rate-of-change statistical values for different coastline positions around the shorelines of Kuala Rompin, Pahang. The Google Earth Engine (GEE) platform obtained the remote sensing data.

This study utilises the GEE platform, a cloud-based computing system that offers efficient methods for storing, retrieving, and analysing datasets on powerful computers (Amani et al., 2020). Cloud-based systems like GEE provide users with various infrastructure, platforms, storage services, and software applications in multiple forms (Chi *et al.*, 2016). GEE integrates Google's computational systems, granting users access to open-access Remote Sensing data (Gorelick *et al.*, 2017). It can automatically execute multiple tasks simultaneously and features a fast-computing system designed to effectively handle the challenges of processing massive amounts of data. Additionally, GEE incorporates a variety of pre-existing algorithms, such as classification algorithms, that can assess data on a global scale (Amani *et al.*, 2019).

The ongoing data processing started in the second phase and continued in the third and fourth stages. The initial phase involves utilising supervised classification to process the data obtained from Landsat and Sentinel Images spanning 2003 to 2023, with the assistance of GEE. The Normalised Difference Water Index (NDWI) detects water features by utilising bands 2 and 4 of Landsat-7 and 3 and 5 for Sentinel-2 images. The Normalised Difference Water Index (NDWI) places a numerical value of zero on bodies of water on the land surface. In contrast, non-water regions on the land surface are assigned values less than or equal to zero (Das *et al.*, 2021). The following equation has been applied to calculate the NDWI value from the Landsat and Sentinel data:

$$\text{NDWI} = \frac{\rho(\lambda\text{g}) - \rho(\lambda\text{nir})}{\rho(\lambda\text{g}) - \rho(\lambda\text{nir})} \qquad (1)$$

where:
$\rho(\lambda\text{g})$ = spectral reflectance of green wavelength
$\rho(\lambda\text{nir})$ = spectral reflectance of near-infrared wavelength

2.2 Shoreline Analysis (DSAS)

This research employed ESRI ArcGIS software to analyse shoreline changes over time, with the Digital Shoreline Analysis System (DSAS) v5 serving as an additional extension to enhance the analysis. With the help of the DSAS software, a method to accurately establish measurement locations, perform rate calculations, and provide statistical data was vital in assessing the shoreline durability rate.

The quantification of shoreline differences using DSAS is commonly achieved through the "baseline and transect" technique. In this method, the user establishes a baseline inside the GIS environment and then casts transect lines perpendicular to the baseline (Gómez-Pazo *et al.*, 2022). The shoreline change rates were determined using two techniques incorporated into the DSAS. The DSAS establishes orthogonal transects along the coast and calculates changing statistics using six unique methods, including End Point Rate (EPR), Net Shoreline Movement (NSM), and Linear Regression Rates (LRR). The EPR statistics are derived by dividing the displacement of the shoreline by the time interval between two specific dates (Yasir *et al.*, 2020). Afterwards, the DSAS model creates transect lines perpendicular to the coastal baseline and intersects the shoreline at the user-select spacing. Each point where the transect intersects the shoreline along this baseline was then used to calculate the rate-of-change statistic (Valderrama-Landeros *et al.*, 2019).

This study employs DSAS software extension to analyse spatial shoreline changes by mapping the rate of coastline movement and changes over a long period. This analysis enables a detailed understanding of the extent of shoreline changes that might not be apparent to the naked eye. Additionally, the study enhances traditional methodology by integrating the GEE platform, leveraging its powerful cloud-based computing capabilities for more efficient data processing and comprehensive geospatial analysis. This combined approach provides a more sophisticated and precise assessment of coastal erosion and shoreline dynamics.

2.3 Shoreline Categorisation

The data used for this study was retrieved from Google Earth Engine, which provided the past and latest satellite imagery intended to enhance the knowledge of the extent and pattern of coastal erosion in the coastline region of Kuala Rompin. This research has used a unique and comprehensive method to discover, analyse and predict the erosion rate of the Kuala Rompin area over 20 years, from 2003 until 2023.

The next step involved was doing a coastal analysis that utilised the processed Landsat and Sentinel data to assess the extent of shoreline erosion that has occurred in recent years, using the statistics given by the DSAS tool. The erosion severity is classified into five categories on a scale ranging from 'High Erosion' to 'High Accretion'. For instance, a rapidly eroding section of shoreline was designated as a "High Erosion" erosion site. Conversely, a shoreline gradually wearing away was selected as a "Stable" erosion site.

The last phase was the erosion rate categorisation of the shoreline analysis, where this phase corresponded to the third objective of this study. The primary interest of this research was to determine and assess the coastal erosion vulnerability rate in Malaysia through coastline extraction and statistical analysis derived from the remote sensing images. This research evaluated and categorised the eroded coastline with the shoreline analysis from the latest remote sensing images.

2.4 Uncertainty Analysis

The standard error of the estimate was typically computed to assess the accuracy of the LRR and Weighted Linear Regression (WLR) procedures. The anticipated value of y, which represented the distance from the baseline, was calculated by utilising the value of x for the line of best fit, as shown in equation 2 below:

$$y = mx + b \qquad (2)$$

where,
y = predicted distance from baseline
m = rate of change
b = y-intercept

Afterwards, the following equation was applied to compute the standard error for LRR, referred to as Linear Regression Standard Error (LSE), and Weighted Regression Rate (WRR), referred to as WSE:

$$LSE\ or\ WSE\ = \sqrt{\frac{\sum(y-y')^2}{n-2}} \qquad (3)$$

where,
y = measured distance from a baseline point for a data point on the shoreline
y' = predicted value derived from the equation
n = number of shorelines used

The R-square statistic was defined as the LR2 for linear regression with one independent variable and the WR2 for weighted linear regression. The equation for the R-square value was determined using:

$$R^2 = 1 - \sqrt{\frac{\sum(y-y\prime)^2}{\sum y - mean\ of y}} \qquad (4)$$

where,

R^2 = coefficient of dependence
y = distance measured from a baseline.
y' = predicted displacement from the baseline
mean of y = average of the measured distance of the shoreline from the baseline.

The equation below was used to obtain an uncertainty value of 0.74 for all the transects, which is referred to as EPRunc (Uncertainty of EPR).

$$EPRunc = \frac{\sqrt{((unc\ A)^2 + ((unc\ B)^2}}{date\ A - date\ B} \qquad (5)$$

where,
unc A= uncertainty from shoreline A
unc B = uncertainty from shoreline B
date A = date of the latest shoreline
date B = date of the oldest shoreline

3.0 Results and Discussion

3.1 Results Obtained from GEE

This section examined and discussed the findings of this study. The 2003, 2013, and 2023 data were analysed using Landsat and Sentinel images acquired via the GEE platform. The abovementioned images were analysed to assess coastal erosion. The surface reflectance dataset of Landsat-7 and Sentinel-2 was utilised due to its already existent atmospheric correction, removing the requirement for additional atmospheric correction.

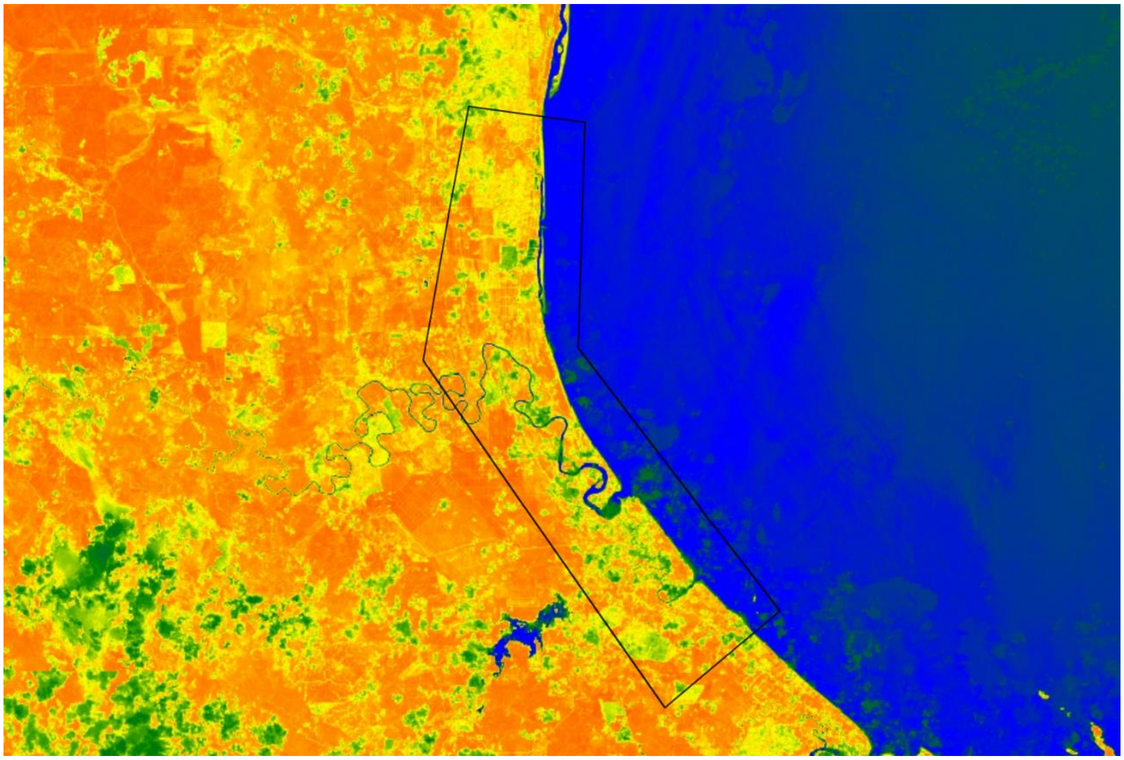

Figure 3. Supervised Classified image of the area

Following that, the shoreline of this region was extracted from the processed images by distinguishing the land cover and area of water through the application of the NDWI index (see Figure 3). The 2003, 2013, and 2023 shorelines were identified and digitised using the DSAS plugin within the GIS software. The findings derived from the coastline rate statistics produced by GIS software were evaluated to see if the shoreline exhibits significant erosion. Figure 4 below demonstrates the shorelines that appeared in 2003, 2013 and 2023, respectively.

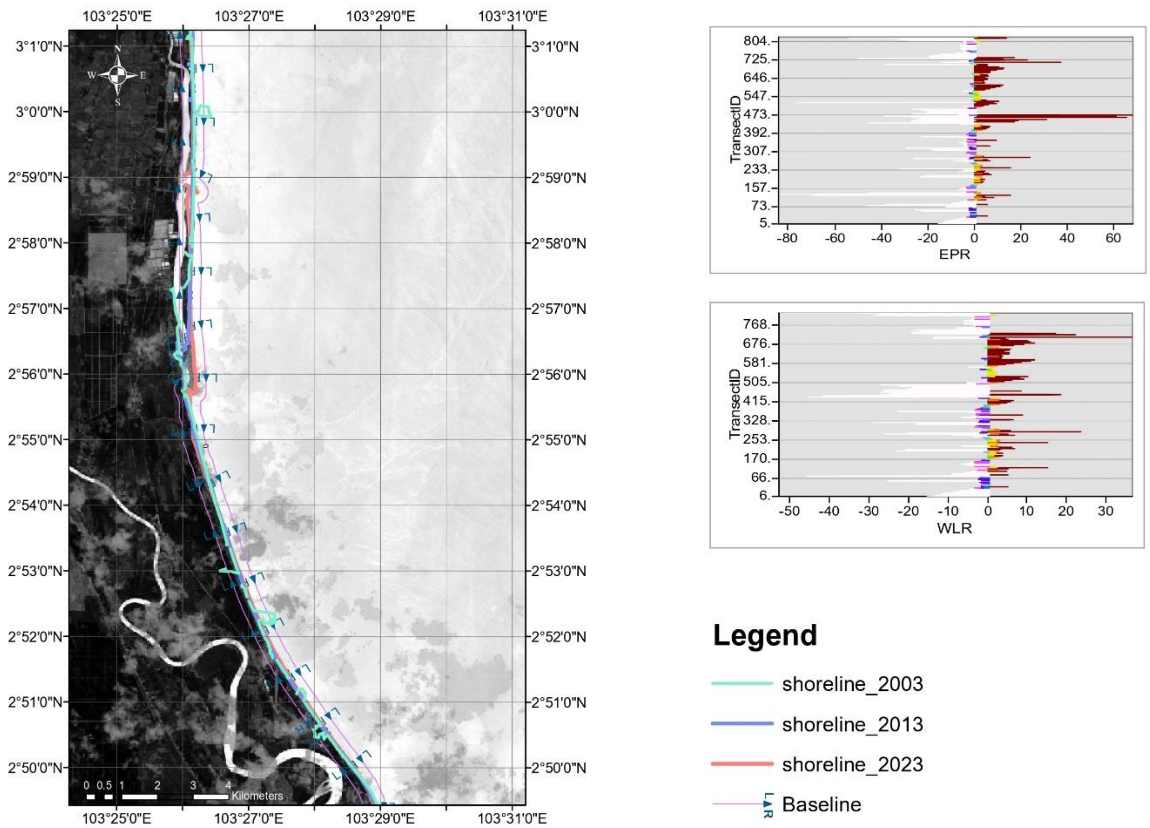

Figure 4. Shorelines from 2003 to 2023

3.2 Shoreline Analysis and Categorisation

The shoreline changes were calculated using EPR, LRR, Shoreline Change Envelope (SCE), and NSM methods for each transect. The figures below present the findings of these study findings. The study conducted a long-term change analysis spanning 20 years (2003-2023). The baseline was considered to be the shoreline of 2003. A total of 795 transects were generated, each spanning a distance of 150 m, encompassing the whole territory. Figures 5 to 8 depict the graphical depiction of the rate changes between 2012 and 2021 for all methods. Figure 9 displays line graph illustrating the rate of changes based on the erosion levels.

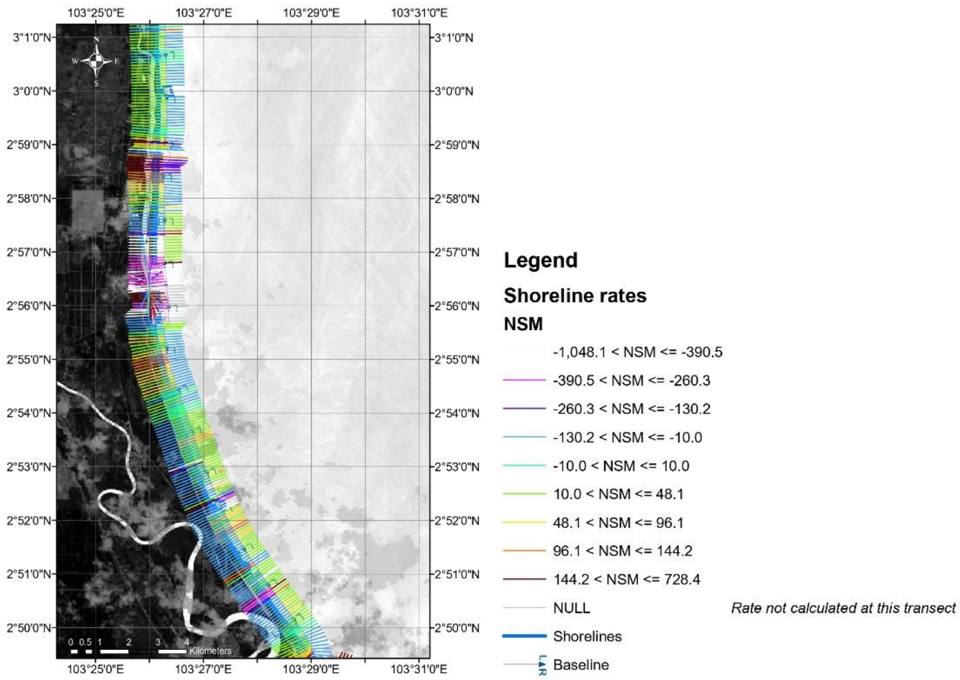

Figure 5. Net Shoreline Movement (NSM) map 2003-2023

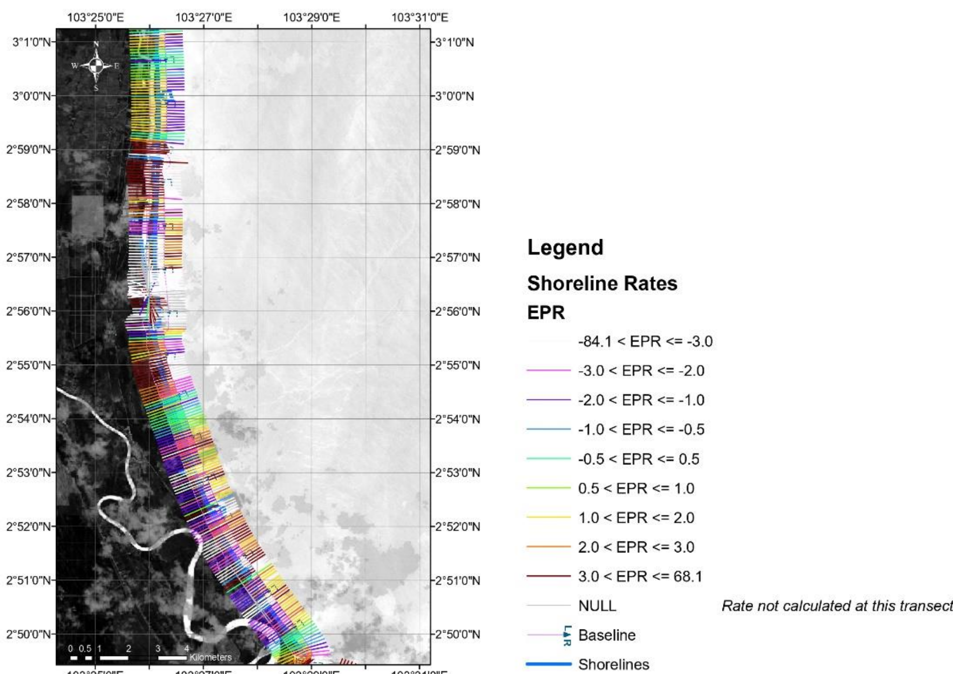

Figure 6. End Point Rate (EPR) map 2003-2023

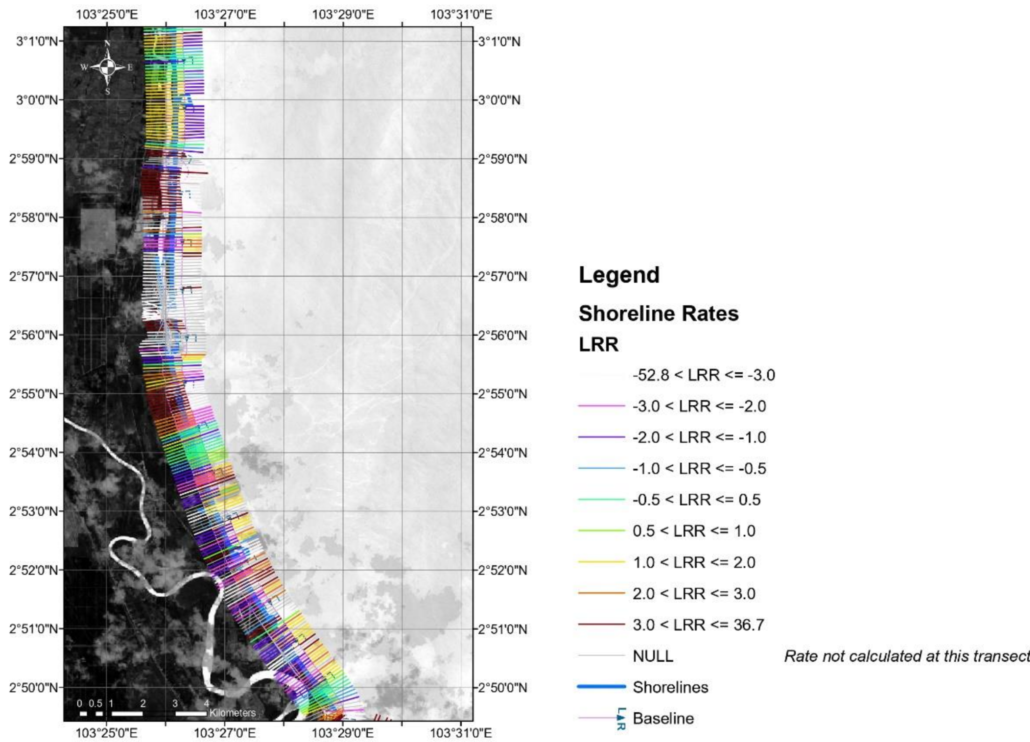

Figure 7. Linear Regression Rate (LRR) map 2003-2023

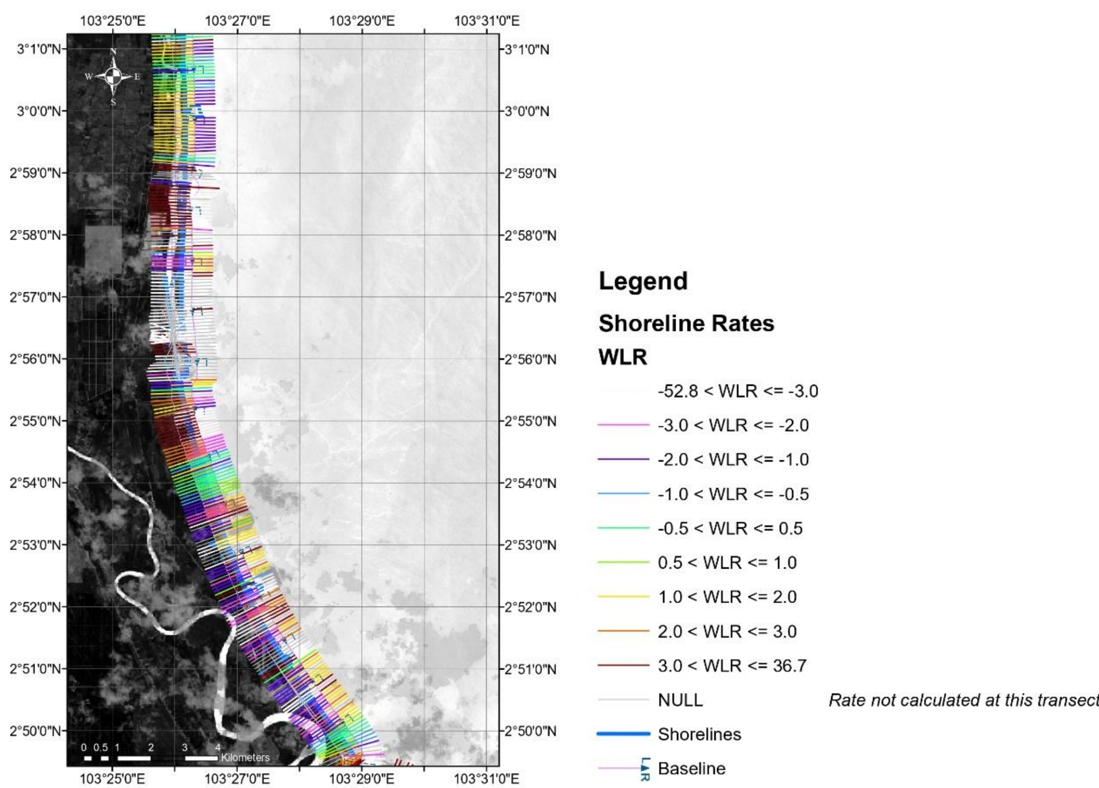

Figure 8. Weighted Linear Regression (WLR) map 2003-2023

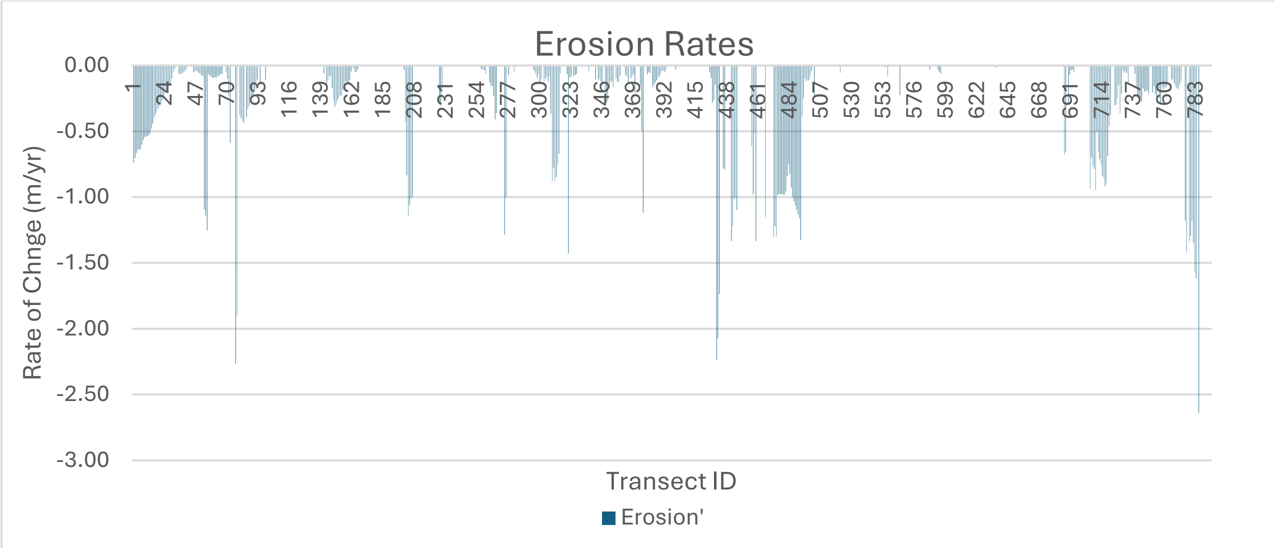

Figure 9. Graph showing the erosion rates

The LRR, EPR, NSM, and SCE values were computed for these transects, and statistical analysis was performed with a 95.5% confidence interval for this data (Table 1). The study examined the rates of accretion and erosion in various areas.

Table 1. Chainage measurement of the attributes along Transect 1-14

ID	SCE	NSM	EPR	EPRunc	LRR	LR2	LSE	WLR	WR2	WSE
1.00	84.16	-84.16	-8.58	0.11	0.00	0.00	0.00	0.00	0.00	0.00
2.00	292.96	-292.96	-14.80	0.05	-14.80	1.00	9.47	-14.80	1.00	12.80
3.00	278.70	-278.70	-14.08	0.05	-14.08	1.00	11.71	-14.08	1.00	15.83
4.00	263.32	-263.32	-13.30	0.05	-13.30	1.00	9.29	-13.30	1.00	12.56
5.00	253.92	-253.92	-12.83	0.05	-12.83	1.00	10.18	-12.83	1.00	13.76
6.00	252.72	-252.72	-12.77	0.05	-12.77	0.99	15.00	-12.77	0.99	20.27
7.00	250.98	-250.98	-12.68	0.05	-12.68	0.99	19.54	-12.68	0.99	26.40
8.00	237.50	-237.50	-12.00	0.05	-12.00	0.99	19.28	-12.00	0.99	26.05
9.00	224.69	-224.69	-11.35	0.05	-11.36	0.99	18.81	-11.36	0.99	25.42
10.00	214.89	-214.89	-10.85	0.05	-10.86	0.99	16.82	-10.86	0.99	22.73
11.00	214.35	-214.35	-10.83	0.05	-10.83	1.00	5.25	-10.83	1.00	7.10
12.00	212.18	-212.18	-10.72	0.05	-10.72	1.00	4.52	-10.72	1.00	6.11
13.00	210.35	-210.35	-10.63	0.05	-10.62	0.99	13.34	-10.62	0.99	18.03
14.00	204.08	-204.08	-10.31	0.05	-10.30	0.99	15.98	-10.30	0.99	21.60

In Table 1, positive numbers indicate accretion, while negative values indicate erosion. Furthermore, taking into account all the transects, it is evident that there are positive averages, indicating accretion. The NSM value measures the magnitude and direction of nett shore movement to the baseline. The SCE value represents the maximum distance between any shoreline intersecting a specific segment. The rate of shoreline change (measured in metres per year) was determined using WLR and EPR statistics (refer to Table 1).

Figure 10 displays a comparative graph illustrating each segment's results of the EPR and LRR approaches. Both approaches yielded comparable outcomes, as was noted. Upon calculating the correlation between these two methodologies, it was determined that there was a 99% relationship. The correlation value demonstrates that both strategies yield consistent results.

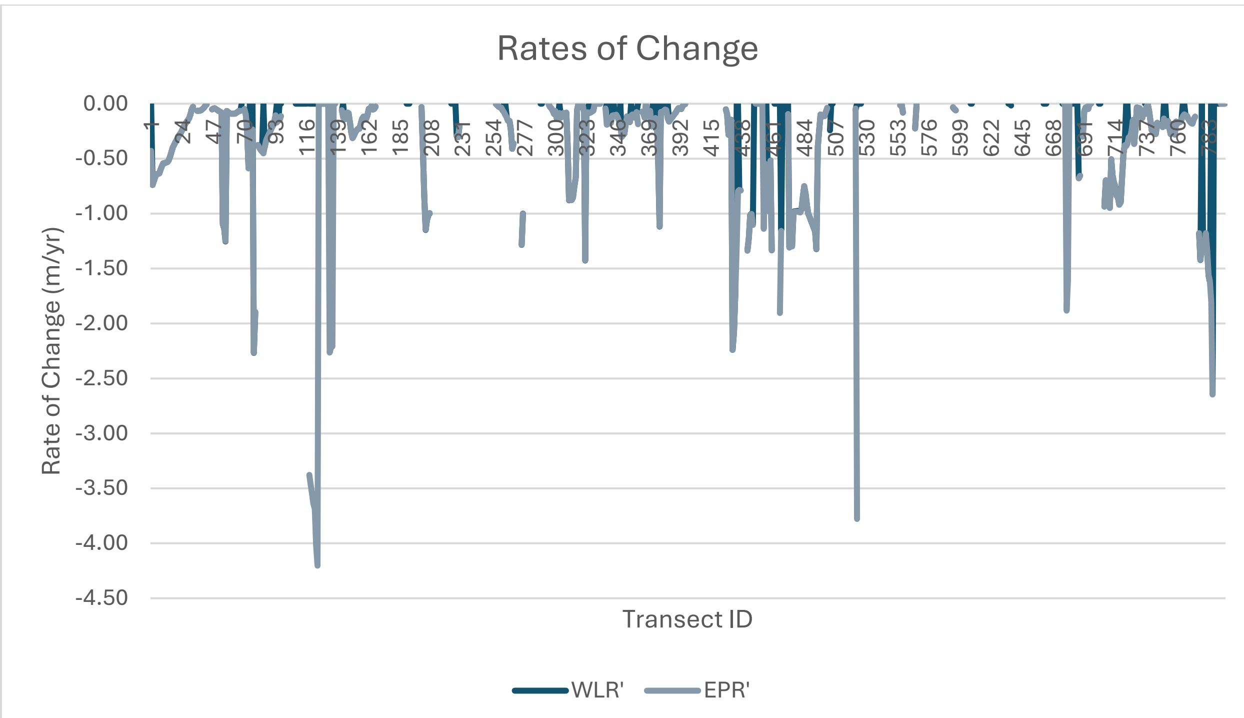

Figure 10. The WLR and EPR values (in m/yr) were calculated for all 795 transects throughout the time from 2003 to 2023

The statistical data from Table 2 shows that the shoreline from 2003 until 2023 has eroded up to 42.89%. The average erosion rate for this period is -0.17 m/yr.

Table 2. Analysis results of the shoreline

	2003-2023
Total Transect	795.00
Total Erosional Transect	341.00
Erosional Transect (%)	42.89
Mean Shoreline Change (m/yr)	-0.09
Max Shoreline Change (m/yr)	1.84
Min Shoreline Change (m/yr)	-2.64
Mean Erosion (m/yr)	-0.17
Standard Deviation Erosion (m/yr)	0.35

Based on the calculated mean erosion rate from the table above, it is evident that the coastline has been undergoing erosion at a rate of -1.88 m/yr throughout the last 20 years. In addition, during the period from 2003 to 2023, the highest rates of erosion are observed in the neighbourhood of regions A, B and C, as depicted in Figure 11 below, with values of -2.27 m/year and -2.24 m/year and -2.64 m/yr, respectively. Kuala Rompin is especially prone to erosion in these specific locations.

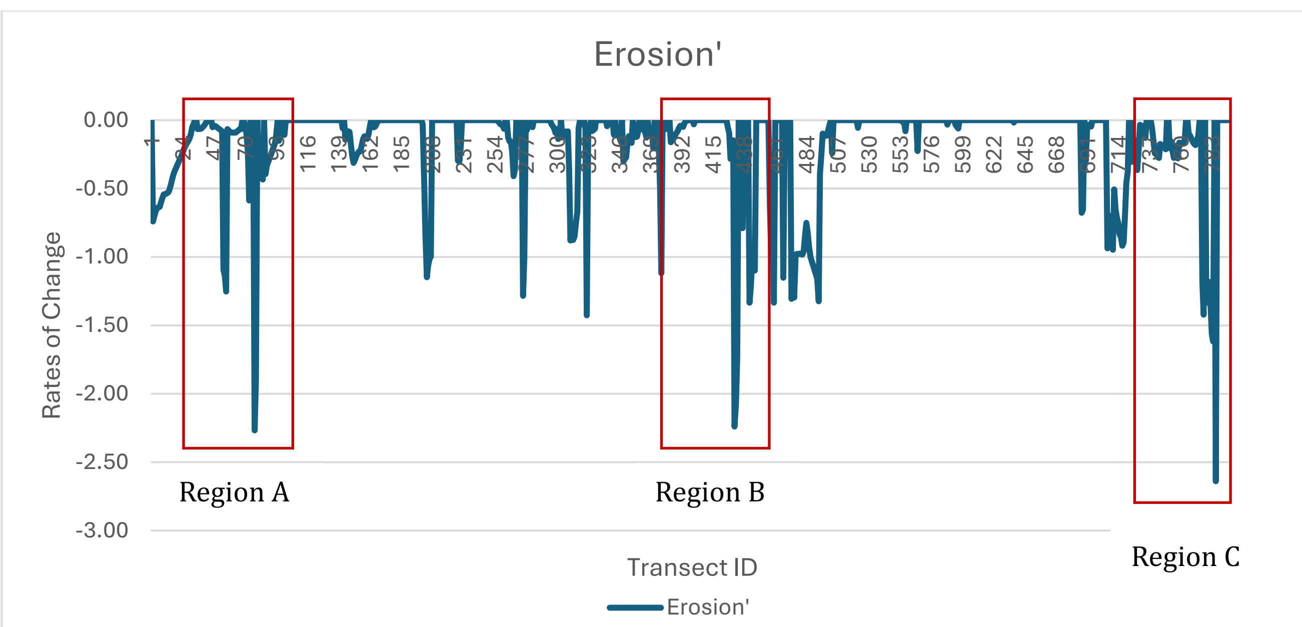

Figure 11. The line graph illustrates the variations in rates across different areas

3.3 Shoreline Accuracy Assessment

The accuracy of LRR and WLR was assessed using R-Square statistics, and the Standard Error of Estimation was also calculated for these rates. Table 3 displays the rate of change for each transect, along with their corresponding accuracy and standard error of estimation values. LR^2 and WR^2 are the coefficients of determination for LRR and WLR, respectively. LSE stands for the standard error of LRR, while WSE stands for the standard error of WLR. The R-square values have been classified into four categories: $R^2 > 0.6$ indicates high accuracy, $R^2 = 0.4 - 0.6$ indicates moderate accuracy, $R^2 < 0.4$ indicates low accuracy, and an R^2 value of 0 implies no link between variables. Under the LRR approach, approximately 60% of the data falls within the high accuracy range, utilising both the WLR and LRR methods. Only about 22% of the data has been identified with a zero R-squared numerical value. Table 3 displays the categorisation of R^2 values together with their corresponding percentages.

Table 3. Accuracy class of shoreline change analysis

	LR^2	LR^2 (%)	WR^2	WR^2 (%)
High Accuracy	474.00	59.62	474.00	59.62
Moderate Accuracy	57.00	7.17	57.00	7.17
Low Accuracy	56.00	7.04	56.00	7.04
No Relation	174.00	21.89	174.00	21.89

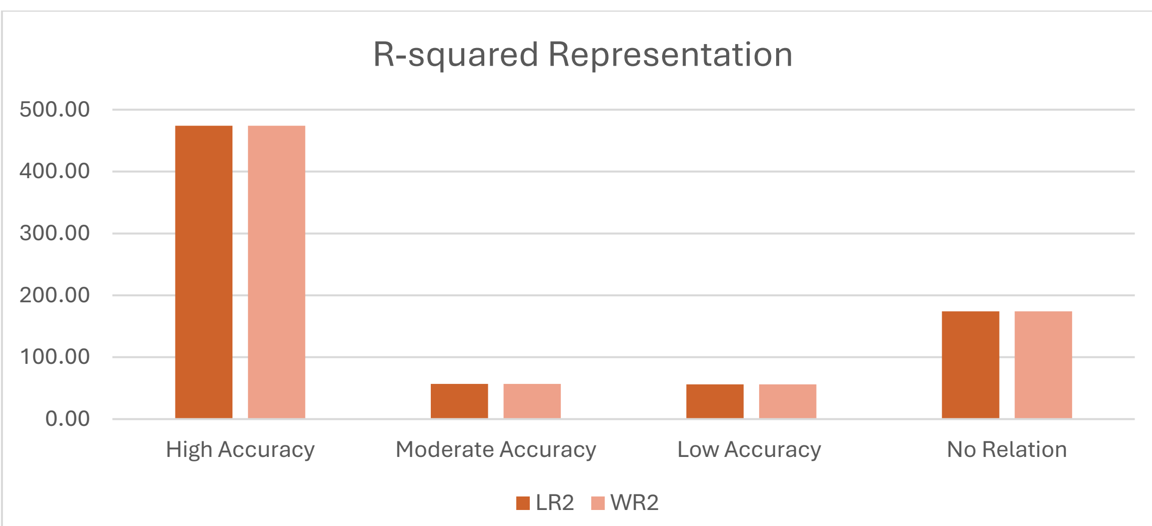

Figure 12. The bar graph that illustrates the R^2 statistics of the two methods

3.4 Coastal Erosion Categorisation

Based on the data from Table 3, it is evident that the shoreline is experiencing an average landward movement at an annual EPR rate of -0.48 m/yr and an annual LRR and WLR rate of -0.39 m/yr. According to the erosion class provided in Table 4, an erosion rate of -0.48 m/yr and -0.39 m/yr is exceptionally high, indicating a significant and rapid loss of shoreline. The extent of erosion is expected to result in substantial land degradation over a relatively brief period, presenting a grave risk to coastal infrastructure, ecosystems, and communities. Immediate action may be necessary in these regions to prevent additional harm and reduce possible hazards, and temporary actions may be required to safeguard vital infrastructure and communities.

Table 4. Average rates of changes 2003-2023

	Average Rate (m/yr)	**Average Erosion Rate (m/yr)**
EPR	-0.14	-0.48
LRR	-0.12	-0.39
WLR	-0.12	-0.39

From this study, regions classified as having “Moderate erosion” underwent a substantial rate of change at their most extreme point. On the contrary, areas classified as “Stable” exhibit a higher average rate of change overall, which is likely attributed to stability in the erosion process. “High erosion” areas exhibit pronounced shifts at their furthest point and a comparably elevated mean value, suggesting a greater degree of persistent erosion around that shoreline area.

Upon analysing the data from Table 5, it is evident that the most significant EPR value is 92.45%, indicating stability. The highest result for WLR is 94.97%, also indicating stability. Based on the data shown in this table, it is evident that although several regions have seen significant erosion, a majority of the shorelines in the study area remain stable, with a few exceptions undergoing moderate erosion. This suggests that erosion is occurring at a rate that does not require immediate intervention, only monitoring in case it worsens.

Table 5. Erosion categorisation classes based on the rates of changes 2003-2023

Class	Values	Total Number of EPR	EPR (%)	Total Number of LRR	LRR (%)	Total Number of WLR	WLR (%)
High erosion	< -4	2.00	0.25	0.00	0.00	0.00	0.00
Moderate erosion	-3.9 - (-1)	58.00	7.30	40.00	5.03	40.00	5.03
Stable	> -1	735.00	92.45	755.00	94.97	755.00	94.97

The erosion observed along this shoreline can be due to the combined effects of waves and tides since this region lacks the presence of islands, which serve as natural barriers to mitigate the impact of waves originating from the open sea. This is further supported by a study by Hugo et al. (2012), which asserts that the shore experiences the direct influence of waves from the South China Sea. The severe erosion can also be due to the increasing demand for urban infrastructure; coastal settings are being transformed to accommodate industrial, residential, and tourism purposes. For example, while severe erosion has happened in multiple study area sites, a former resort that was famous for being a tourist destination named Summerset Resort, Rompin, had seen the most substantial damage. The buildings constructed in this area have crumbled, resembling the force of a 'tsunami' during the past five to six years. The incident is thought to have occurred due to haphazard development constructed close to the beach without considering the potential long-term consequences, such as the impact of waves (Aziz, 2024).

While infrastructure is crucial in supporting the growing human population, too much of it can also cause severe environmental damage (Arriffin *et al.*, 2023). The rise in population can harm the coastal ecosystem due to densely populated regions, which may further worsen erosion levels in the study area.

4.0 Conclusion

The primary objective of this study was to utilise geospatial technology to gain a deeper understanding of the shoreline change rate and assess the magnitude of coastal erosion in the Kuala Rompin shoreline area. Erosion exhibits significant variability due to semi-diurnal and mixed tides with an extensive tidal range, which human activities and global warming have recently amplified. The research region's coastline geomorphology is significantly altered by extensive erosion. The vast mudflats region is experiencing increased erosion due to its soft underlying sediments. Another consequence of erosion is the alteration of regional hydrodynamics. Given the significant human impact on the study area and its designation as a hub for major human activities, it is crucial to conduct a thorough examination of the stability of mudflats, the rate at which sediment is transported, and the ability to anticipate future changes in the shoreline of the study region. This is necessary to promote sustainable development. The three rate calculation methods, EPR, LRR, and WLR, are significant since EPR allows for rapid measurement and straightforward calculation. In contrast, LRR and WLR are more dependable as they are entirely based on known statistical concepts, making them undeniably computational.

This research has showcased a flexible and adaptable framework for evaluating the susceptibility of coastal areas over 20 years. This extended long-term timeframe allows researchers to capture the natural variability and cyclical patterns of coastal processes and detect the gradual, cumulative impacts of factors such as climate change, sea-level rise, and human activities on the coastline. The analysis of the shoreline data from 2003 to 2023 indicates an average erosion rate of -0.48 m/yr using the EPR method and -0.39 m/yr using the LRR and WLR methods. This erosion has been particularly severe in specific regions, with the highest rates reaching up to -2.64 m/yr. These findings provide valuable insights that can inform sustainable development and coastal management strategies for the Kuala Rompin shoreline, which is facing increasing pressures from natural phenomena and human activities.

The findings in this study serve as a crucial reference for environmental scientists, policymakers, and coastal managers. Therefore, the study recommends implementing regular and systematic monitoring programs, promoting sustainable development practices, adopting integrated coastal management approaches, increasing public awareness and education about coastal erosion, and developing predictive models to anticipate future changes in the shoreline.

Acknowledgement

The authors would like to express their sincere gratitude to Universiti Teknologi Malaysia (under research votes PY/2024/00639) and grant number Q.J130000.3852.42J12 for sustaining this project as well as all the parties who helped this research.

References

Amani, Meisam, Sahel Mahdavi, Majid Afshar, Brian Brisco, Weimin Huang, Sayyed Mohammad Javad Mirzadeh, Lori White, Sarah Banks, Joshua Montgomery, and Christopher Hopkinson. (2019). "Canadian Wetland Inventory using Google Earth Engine: The First Map and Preliminary Results" *Remote Sensing* 11, no. 7: 842. https://doi.org/10.3390/rs11070842

Apostolopoulos, D., & Nikolakopoulos, K. (2021). A review and meta-analysis of remote sensing data, GIS methods, materials and indices used for monitoring the coastline evolution over the last twenty years. *European Journal of Remote Sensing*, *54*(1), 240-265.

Ariffin, E. H., Mathew, M. J., Roslee, A., Ismailluddin, A., Yun, L. S., Putra, A. B., ... & Lee, L. H. (2023). A multi-hazards coastal vulnerability index of the east coast of Peninsular Malaysia. *International Journal of Disaster Risk Reduction*, *84*, 103484.

Castelle, B., & Harley, M. (2020). Extreme events: impact and recovery. In *Sandy Beach morphodynamics* (pp. 533-556). Elsevier.

Das, T., Jana, A., Mandal, B., & Sutradhar, A. (2021). S patio-temporal pattern of land use and land cover and its effects on land surface temperature using remote sensing and GIS techniques: A case study of Bhubaneswar city, Eastern India (1991–2021). *GeoJournal*, 1-31.

Dionysios Apostolopoulos & Konstantinos Nikolakopoulos (2021), A review and meta-analysis of remote sensing data, GIS methods, materials and indices used for monitoring the coastline evolution over the last twenty years, European *Journal of Remote Sensing*, 54:1, 240-265, DOI: 10.1080/22797254.2021.1904293

Effi Helmy Ariffin, Manoj Joseph Mathew, Adina Roslee, Aminah Ismailluddin, Lee Shin Yun, Aditya Bramana Putra, Ku Mohd Kalkausar Ku Yusof, Masha Menhat, Isfarita Ismail, Hafiz Aiman Shamsul, David Menier, Nor Hisham M. Ghazali, Lee Hin Lee, (2023), A multi-hazards coastal vulnerability index of the east coast of Peninsular Malaysia, International Journal of Disaster Risk Reduction, 103484, ISSN 2212-4209, https://doi.org/10.1016/j.ijdrr.2022.103484

Gómez-Pazo, A., Payo, A., Paz-Delgado, M. V., & Delgadillo-Calzadilla, M. A. (2022). Open digital shoreline analysis system: ODSAS v1. 0. *Journal of Marine Science and Engineering*, *10*(1), 26.

Gorelick, N., Hancher, M., Dixon, M., Ilyushchenko, S., Thau, D., & Moore, R. (2017). Google Earth Engine: Planetary-scale geospatial analysis for everyone. *Remote sensing of Environment*, *202*, 18-27.

Hasan, R. C., Irtem, E., & Kabdaşlı, M. S. (2023). Coastal erosion vulnerability along Malaysia's major sedimentary basins. *Ocean & Coastal Management, 242*, 106712.

Hugo, G., Bardsley, D., Sharma, V., Tan, Y., Williams, M., & Bedford, R. (2012). Addressing climate change and migration in Asia and the Pacific.

Hussaini, A., Mahmud, M. R., & Tang, K. K. W. (2020, July). Change Detection for the Past Three Decades Using Geospatial Approach in Lake Chad, Central Africa. In *IOP Conference Series: Earth and Environmental Science* (Vol. 540, No. 1, p. 012001). IOP Publishing.

Hussaini, A., Mahmud, M. R., Tang, K. K. W., & Abubakar, A. G. (2019). Water level fluctuation assessment of Lake Chad for environmental sustainability using remote sensing and geographic information system technique. *The International Archives of the Photogrammetry, Remote Sensing and Spatial Information Sciences*, *42*, 261-266.

Ilah Hafiz Aziz, Amin Ridzuan Ishak (September, 2017), Pantai Hilang 4 Meter Setahun, Accessed 01 June 2024, https://www.bharian.com.my/berita/nasional/2017/09/323870/pantai-hilang-4-meter-setahun. Last accessed on 1st June 2024.

Mahmud, M. R., & Tang, K. K. W. (2023). Challenges Of Nearshore Bathymetric Mapping Using Satellite Derived Bathymetry In Malaysia. In *FIG working week 2023*.

Masselink, G., & Gehrels, R. (2014). *Coastal environments and global change*. John Wiley & Sons.

McClenachan, G. M., Donnelly, M. J., Shaffer, M. N., Sacks, P. E., & Walters, L. J. (2020). Does size matter? Quantifying the cumulative impact of small-scale living shoreline and oyster reef restoration projects on shoreline erosion. *Restoration Ecology*, *28*(6), 1365-1371.

Meisam Amani , Senior Member, Arsalan Ghorbanian , Seyed Ali Ahmadi , Mohammad Kakooei, Armin Moghimi , S. Mohammad Mirmazloumi, Student Member, Sayyed Hamed Alizadeh Moghaddam , Sahel Mahdavi, Masoud Ghahremanloo, Saeid Parsian, Qiusheng Wu , and Brian Brisco., (2020), "Google Earth Engine Cloud Computing Platform for Remote Sensing Big Data Applications: A Comprehensive Review," in *IEEE Journal of Selected Topics in Applied Earth Observations and Remote Sensing*, vol. 13, pp. 5326-5350, doi: 10.1109/JSTARS.2020.3021052

Mohamed Rashidi, A.H. (2021, July 02). Coastal Structures in Malaysia. In Encyclopedia. https://encyclopedia.pub/entry/11596. Last accessed on 1st June 2024.

Mohamed Rashidi, A. H., Jamal, M. H., Hassan, M. Z., Mohd Sendek, S. S., Mohd Sopie, S. L., & Abd Hamid, M. R. (2021). Coastal Structures as Beach Erosion Control and Sea Level Rise Adaptation in Malaysia: A Review. *Water*, *13*(13), 1741. MDPI AG. Retrieved from http://dx.doi.org/10.3390/w13131741. Last accessed on 1st June 2024.

M. Chi, A. Plaza, J. A. Benediktsson, Z. Sun, J. Shen and Y. Zhu, (Nov. 2016), "Big data for remote sensing: Challenges and opportunities", *Proc. IEEE*, vol. 104, no. 11, pp. 2207-2219.

M. Yasir et al., "Automatic Coastline Extraction and Changes Analysis Using Remote Sensing and GIS Technology," in *IEEE Access*, vol. 8, pp. 180156-180170 (2020), doi: 10.1109/ACCESS.2020.3027881, https://ieeexplore.ieee.org/abstract/document/9210098. Last accessed on 1st June 2024.

N. Gorelick, M. Hancher, M. Dixon, S. Ilyushchenko, D. Thau and R. Moore, (Dec 2017), "Google earth engine: Planetary-scale geospatial analysis for everyone", *Remote Sens. Environ.*, vol. 202, pp. 18-27.

Thieler, E. R., Himmelstoss, E. A., Zichichi, J. L., & Ergul, A. (2009). *The Digital Shoreline Analysis System (DSAS) version 4.0-an ArcGIS extension for calculating shoreline change* (No. 2008-1278). US Geological Survey.

Turner, I. L., Harley, M. D., Short, A. D., Simmons, J. A., Bracs, M. A., Phillips, M. S., & Splinter, K. D. (2016). A multi-decade dataset of monthly beach profile surveys and inshore wave forcing at Narrabeen, Australia. *Scientific data*, *3*(1), 1-13.

Luijendijk, A., Hagenaars, G., Ranasinghe, R., Baart, F., Donchyts, G., & Aarninkhof, S. (2018). The state of the world's beaches. *Scientific reports*, 8(1), 6641.

Valderrama-Landeros, L., & Flores-de-Santiago, F. (2019). Assessing coastal erosion and accretion trends along two contrasting subtropical rivers based on remote sensing data. *Ocean & Coastal Management*, *169*, 58-67.

Wan-Afnizan, W. M., Al-Qadami, E. H. H., Razi, M. A. M., Aminon, N. A., Mahamud, M., & Aziz, A. (2024, June). Detection of mainland Kedah's shoreline changes (2013-2020); a case study. In *IOP Conference Series: Earth and Environmental Science* (Vol. 1347, No. 1, p. 012017). IOP Publishing.